



## (3) Magnetization Process

### □ Uniaxial Magnetization

**Hard-axis Magnetization**

**Easy-axis Magnetization**

### □ Field at Arbitrary Orientation to Uniaxial Easy Axis

**Stoner-Wohlfarth Problem**

**Magnetization Change by Curling**

**Free Domain Walls**

**Approach to Saturation**

### □ Domain Wall Pinning and Coercivity

**Large “Fuzzy” Defects**

**Micromagnetic Theory for Well-defined Defects**

**Examples**

**Additional Anisotropy**

# (3) Magnetization Process

## Uniaxial Magnetization

(Origin of uniaxial anisotropy : magnetostatic, magnetocrystalline, magnetoelastic, or field-induced)

$$K_u = (1/2)\mu_o(N_a - N_c)M_s^2 \text{ for magnetostatic (shape)}$$

$$K_{u1} \text{ for magnetocrystalline}$$

$$3\lambda_s\sigma/2 \text{ for magnetoelastic (isotropic)}$$

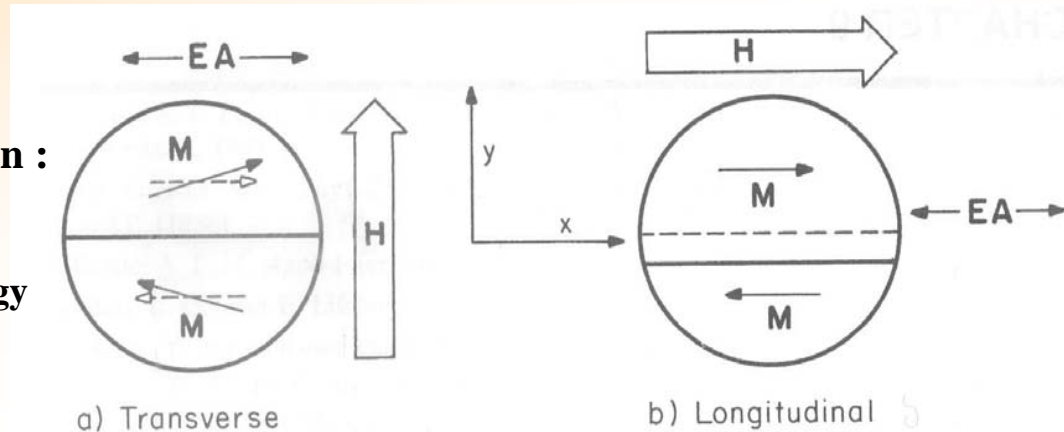


**Figure 9.1.** Schematic representations of a magnetic material having purely uniaxial anisotropy in the direction of the easy axis (EA). Dashed lines indicate magnetization configurations for  $H = 0$ . Application of a field  $H$  transverse to the EA results in rotation of the domain magnetizations but no wall motion. Application of a field parallel to the EA results in wall motion but no rotation of the domain magnetization.

**Hard-axis magnetization :**

**Related magnetic energy**

- Uniaxial anisotropy energy

- Zeeman energy

**Easy-axis magnetization :**

**Related magnetic energy**

- Uniaxial anisotropy energy

- Zeeman energy

# (3) Magnetization Process

## Hard-axis Magnetization (see Fig. 9.1(a) in O'Handley)

For  $H \perp$  easy axis, total energy density

$$f = f_a + f_{Zeeman} = K_u \sin^2(\pi/2 - \theta) - \mathbf{M}_s \cdot \mathbf{B}$$

$$= K_u \cos^2 \theta - M_s H \cos \theta, \quad K_u > 0$$

Torque,  $T_\theta = -\partial f / \partial \theta$  on  $\mathbf{M}$

Minimum  $f$  when  $\partial f / \partial \theta = (-2K_u \cos \theta + M_s H) \sin \theta = 0$

$$\text{and } \partial^2 f / \partial \theta^2 = -2K_u \cos^2 \theta + M_s H \cos \theta > 0$$

Zero torque:  $\sin \theta = 0 \rightarrow \theta = 0, \pi, \dots$

Stability conditions (see Fig. 2.12 in O'Handley) :

$\theta = 0$  is stable only for  $H > 2K_u / M_s$  ( $K_u > 0$ )

$\theta = \pi$  is stable only for  $H < -2K_u / M_s$  ( $K_u > 0$ )

Equation of motion for the magnetization in fields below saturation ( $-2K_u / M_s < H < 2K_u / M_s$ )

$$2K_u \cos \theta = M_s H$$

For  $H = 0$ ,  $\theta = \pi/2$ ,  $H_a$  (anisotropy field) =  $H_{sat}$  for  $\cos \theta = 1$

Since  $M = M_s \cos \theta$ ,  $K_u = M_s H_a / 2$ , Then  $2K_u \cos \theta = M_s H \rightarrow H_a M_s \cos \theta = M_s H$

Using reduced magnetization,  $m = M / M_s = \cos \theta$  and  $h = H / H_a$

$$m = h \quad \text{for } -1 \leq h \leq 1 \quad (\text{see Fig. 9.2(a) in O'Handley})$$

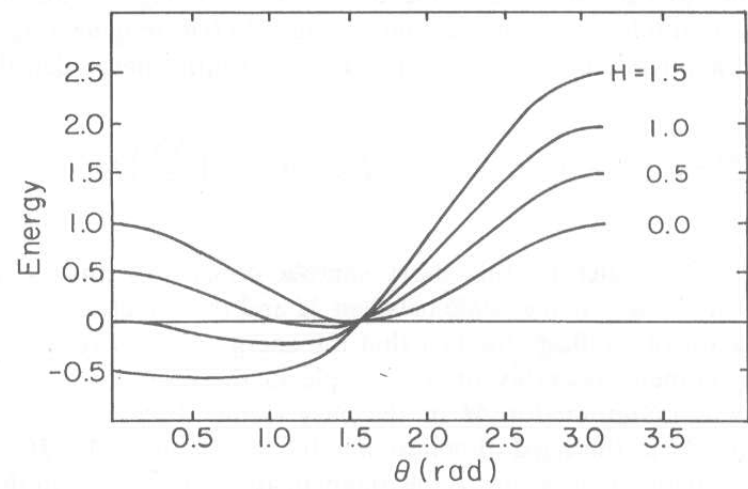


Figure 2.12 Variation of magnetostatic plus Zeeman energy density with  $\theta$  for increasing values of applied field (arbitrary units). Note how the stable energy minimum moves from  $\pi/2$  toward zero as applied field increases.

### (3) Magnetization Process

#### Easy-axis Magnetization (see Fig. 9.1(b) in O'Handley)

Free energy in a single domain particle (or completely pinned wall)

$$f = -M_s H \cos \theta + K_u \sin^2 \theta$$

Energy density  $f$  versus  $\theta$  for various  $h$  (reduced field)  $= M_s H / 2K_u$

Stability conditions:

For  $h = 0$  (i.e., zero field), stable at both  $\theta = 0$  and  $\pi$

For  $0 < h < 1$ , angular position of min.  $f$  is independent of field.

For  $h = 1$ ,  $\theta = \pi$  is no more stable,  $m = 0$  called the *switching field*.

Zero-torque condition:  $M_s H \sin \theta + 2K_u \sin 2\theta = 0$

$$\theta = 0 \ (m = 1) \text{ and } \pi \ (m = -1)$$

Stability conditions:  $M_s H \cos \theta + 2K_u \cos 2\theta > 0$

$\theta = 0$  is stable only for  $H > -2K_u / M_s$  ( $h > -1$ )

$\theta = \pi$  is stable only for  $H < 2K_u / M_s$  ( $h < 1$ )

$\theta = 0$  and  $\pi$  are only *locally stable* for  $-2K_u / M_s < H < 2K_u / M_s$

In Fig. 9.2(b), solid lines : stable solutions

dashed lines : locally stable solutions  $\rightarrow$  square hysteresis loop!!!

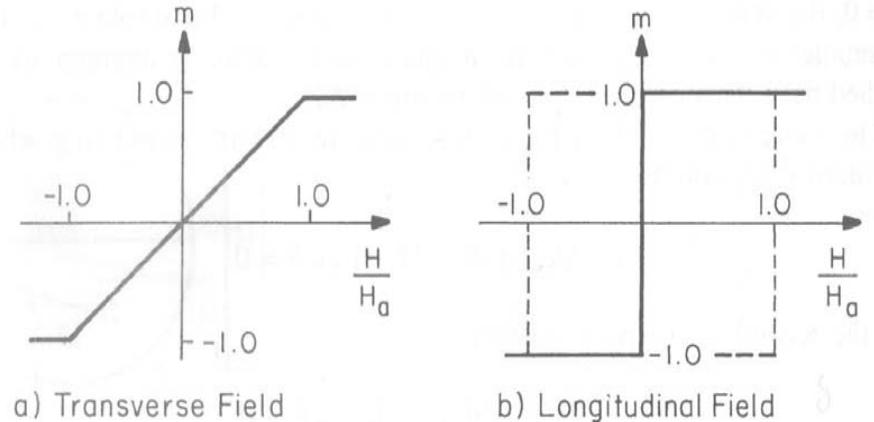


Figure 9.2.  $M$ - $H$  loops for the two idealized cases shown in Figure 9.1: (a) hard-axis and (b) easy-axis magnetization processes.

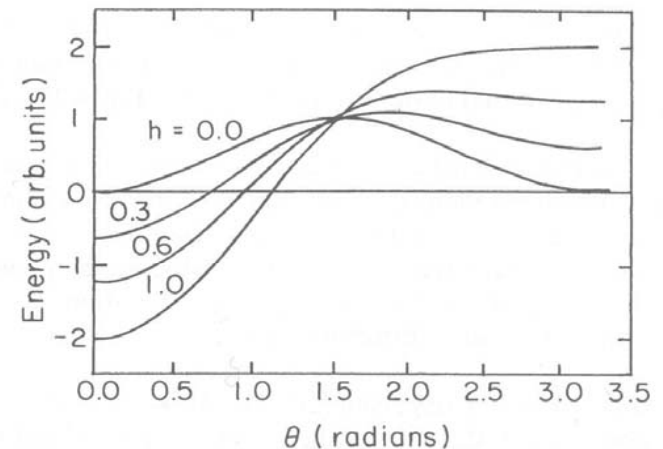


Figure 9.3. Free energy for the easy-axis magnetization process as a function of angle and applied field strength,  $h = M_s H / 2K_u$ .



## (3) Magnetization Process

### Easy-axis Magnetization (continued)

In the case of domain wall motion :

No torque on the domain magnetization, but a torque on the spins making up the wall

- The spins in the wall may rotate to align with  $H$

Macroscopically, the difference in Zeeman energy of the two domains (a field-induced potential energy difference) across the domain wall ( $= 2M_s H$ )  $\rightarrow$  lower energy by moving so as to reduce the volume of the unfavorably oriented domain

Equivalently, the force on the domain wall, given by  $F = -\partial U/\partial x$ , will move the wall down.

Assuming smooth and easy wall motion (negligible pinning), solid line with zero coercivity

(see Fig. 9.2(b) in O'Handley)

Coercive field  $H_c$  :

$H_c = 2K_u/M_s$  in the single-domain or pinned wall limit by rotational hysteresis

$H_c = 0$  in free-domain-wall limit

Permeability  $\mu_{\text{rot}}$  for a purely rotational magnetization process :

$$2K_u \cos \theta = M_s H \rightarrow H_a M_s \cos \theta = M_s H \text{ since } H_c = 2K_u/M_s \text{ and } M = M_s \cos \theta \rightarrow M = (M_s^2/2K_u)H$$

$$\mu_{\text{rot}} = \mu_0(H + M)/H = \mu_0(1 + M_s^2/2K_u) \approx \mu_0 M_s^2/2K_u \text{ (SI unit)} \quad \mu_{\text{rot}} \approx 2\pi M_s^2/K_u \text{ (cgs)}$$

If  $K_u$  is small, the  $M$ - $H$  loop is steep and  $\mu_{\text{rot}}$  can be large!!!

# (3) Magnetization Process

## Field at Arbitrary Orientation to Uniaxial Easy Axis

### Stoner-Wohlfarth Problem :

The magnetization process for single-domain particles of ellipsoidal shape

- The  $M$ - $H$  loops for a field applied at an arbitrary angle  $\theta_0$  with respect to a uniaxial easy axis (see Fig. 9.4 in O'Handley)

For a prolate spheroid, the free energy  $f$

$$f = -K_u \cos^2(\theta - \theta_0) - M_s H \cos \theta$$

where  $K_u = [H_a + (N_2 - N_1)M_s]M_s/2$ ,  $H_a$  is the anisotropy field,  $N_1$  and  $N_2$  are demagnetization factors // and  $\perp$  to the easy axis of the particle, respectively.

Minimum free energy when  $\partial f / \partial \theta = 0$

$$2K_u \sin(\theta - \theta_0) \cos(\theta - \theta_0) + M_s H \sin \theta = 0$$

Using  $K_u = H_a M_s / 2$  and the reduced field  $h = H / H_a$ ,

$$\sin 2(\theta - \theta_0) + 2h \sin \theta = 0$$

With the reduced magnetization  $m = M / M_s = \cos \theta$ , the solution can be written as the following,

$$2m(1 - m^2)^{1/2} \cos 2\theta_0 + (1 - 2m^2) \sin 2\theta_0 \pm 2h(1 - m^2)^{1/2} = 0 \rightarrow h = f(m) \quad (\text{see Fig. 9.5 in O'Handley})$$

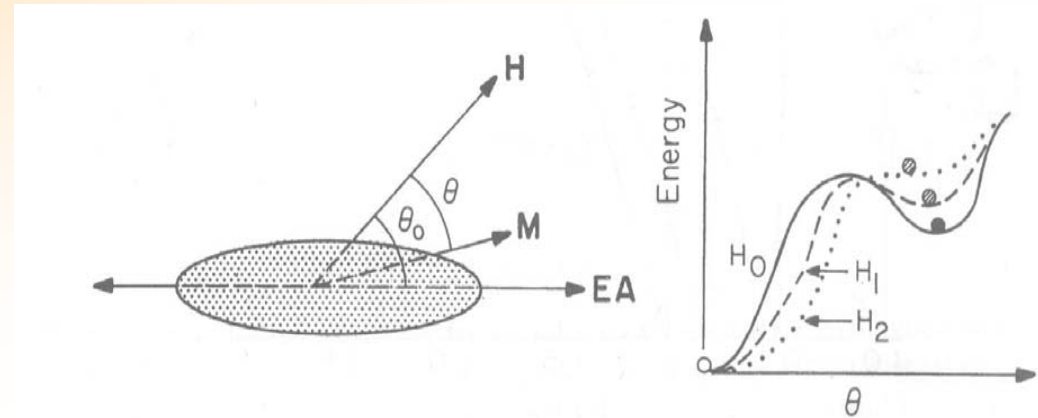


Figure 9.4. Left, coordinate system for magnetization reversal process in single-domain particle in which the shape and crystallographic easy axes coincide. Application of a field at an angle  $\theta_0$  relative to the EA causes a net magnetization to lie at some angle  $\theta$  relative to the field. Right, illustration of approach to a discontinuous magnetization change at a negative field of magnitude  $H_2$ .

### (3) Magnetization Process

Equation of motion for the magnetization :

$$2m(1 - m^2)^{1/2}\cos 2\theta_0 + (1 - 2m^2)\sin 2\theta_0 \pm 2h(1 - m^2)^{1/2} = 0$$

#### Interpretations

- (i)  $\theta_0 = \pi/2$  : Hard-axis magnetization  
(Fig. 9.2(a) in O'Handley)
- (ii)  $\theta_0 = 0$  : Easy-axis magnetization  
(Fig. 9.2(b) in O'Handley)
- (iii) Single-domain, oblique magnetization process  
in negative fields

- For a small range of  $\theta_0$  above  $0^\circ$ ,  
the magnetization reversal occurs at a critical field,  
 $h_s = H_s/H_a$ , called the *reduced switching field*;  
 $h_s$  is defined where  $m(h)$  curve satisfies  $\partial h/\partial m = 0$ .

At the switching point,  
the magnetization switches abruptly and reversibly.  
free energy minimum ( $\partial f/\partial \theta = 0$ ) becomes flat  
(i.e., unstable):  $\partial^2 f/\partial \theta^2 = 0$ .

$$h_s \cos \theta - \cos 2(\theta - \theta_0) = 0 \quad (\text{since } \partial f/\partial \theta = \sin 2(\theta - \theta_0) + 2h \sin \theta)$$

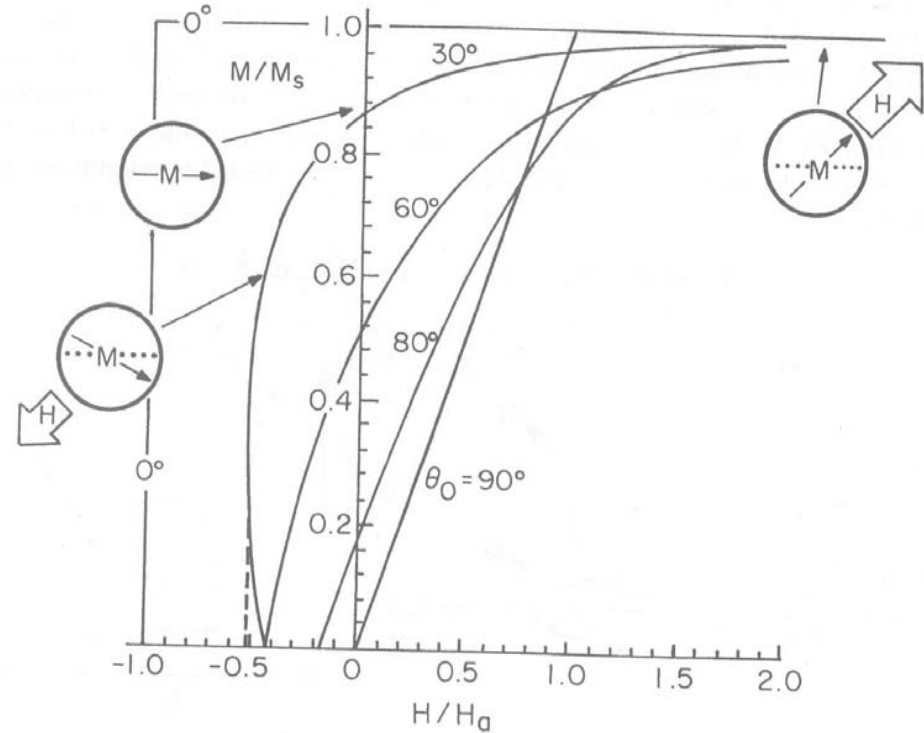


Figure 9.5. Stoner–Wohlfarth (SW) solutions: reduced magnetization versus reduced field applied at an angle  $\theta_0$  to the easy axis. The linear  $m-h$  curve represents  $\theta_0 = 90^\circ$ , and the other curves of increasing remanence represent  $\theta_0 = 80^\circ, 60^\circ$ , and  $30^\circ$ . The magnetization process is irreversible so  $m-h$  continues for  $h < 0$ . Possible magnetization distributions are shown as inserts for nucleation-inhibited, single-domain particles.

### (3) Magnetization Process

#### Explanations (continued)

At the switching point,

$$h_s \cos \theta - \cos 2(\theta - \theta_0) = 0$$

Then

$$\sin 2\theta_0 = (2/h_s^2)[(1 - h_s^2)/3]^{-3/2}$$

Solving for the switching field,

$$h_s = (\cos^{2/3} \theta_0 + \sin^{2/3} \theta_0)^{-3/2}$$

(see Fig. 9.6 in O'Handley)

For  $45^\circ < \theta_0 < 90^\circ$ ,  $h_s$  occurs after the magnetization has changed sign; the coercivity  $h_c$  is less than  $h_s$ . And thus  $h_c$  is defined at  $m = 0$ ,  $h_c = \sin \theta_0 \cos \theta_0$

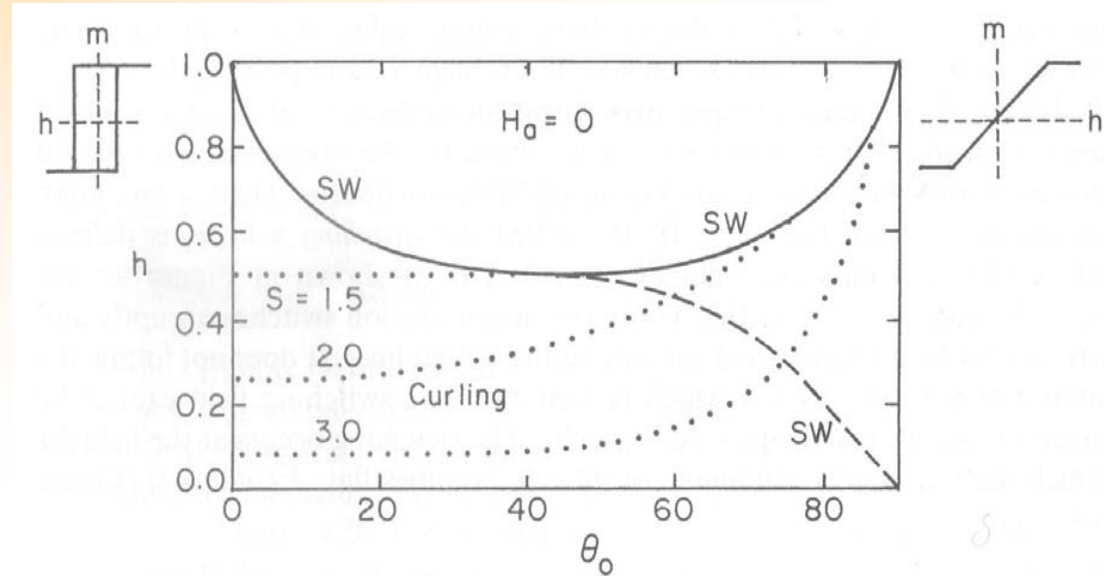


**Figure 9.6.** Solid line: variation of the switching or coercive field,  $h_i = H_i/H_a^{\text{eff}}$ , with angle between easy axis and applied field. The shapes of the  $m$ - $h$  loops at the two extreme values of  $\theta_0$ , are shown for reference. The solid line describes the switching field for the uniform rotation process (SW). For  $\theta_0 > 45^\circ$ , the magnetization passes through zero (defining  $h_c$ ) for fields less negative than the switching field. Dotted lines indicate switching fields for curling, Eq. (9.16), for various values of the reduced minor-axis radius,  $S = b/b_0$ . Magnetocrystalline anisotropy is neglected. The particle aspect ratio for the curling-mode results is 8.



### (3) Magnetization Process

#### Magnetization Change by Curling :

- Modes of magnetization reversal
- (i) Coherent rotation of all moments in unison (see Fig. 9.7(a) in O'Handley)
- (ii) Curling (see Fig. 9.7(b) in O'Handley)
- (iii) Buckling (see Fig. 9.7(c) in O'Handley)
- (iv) Fanning (in chain of spheres) (see Fig. 9.7(d) in O'Handley)
- (v) Domino effect (see Fig. 9.7(e) in O'Handley)

- Magnetization switching by curling

By having fewer spins pointing away from the easy axis at any

given stage of the reversal process, exchange energy is raised and the magnetostatic energy is lowered.

Switching field  $H_s$  for magnetization curling in an elongated, single-domain particle of semiminor axis  $b$  is reduced from the uniform rotation value,  $H_c = (N_b - N_a)M_s$ , by replacing the hard-axis magnetostatic energy with the curling energy,

$$H_s = [(a/2)(b_o/b)^2 - N_a]M_s \propto C_1/b^2 - C_2$$

where  $b_o = r_o/N_b^{1/2}$  is the single-domain radius for an ellipsoid of revolution and  $a$  is a function of the aspect ratio of particles (1.08 (infinite cylinder)  $\leq a \leq$  1.42 (sphere)).

$\theta_o$  dependence of  $H_s$  due to curling for various values of  $S = b/b_o$ , assuming no magnetocrystalline anisotropy

(see Fig. 9.8 in O'Handley).

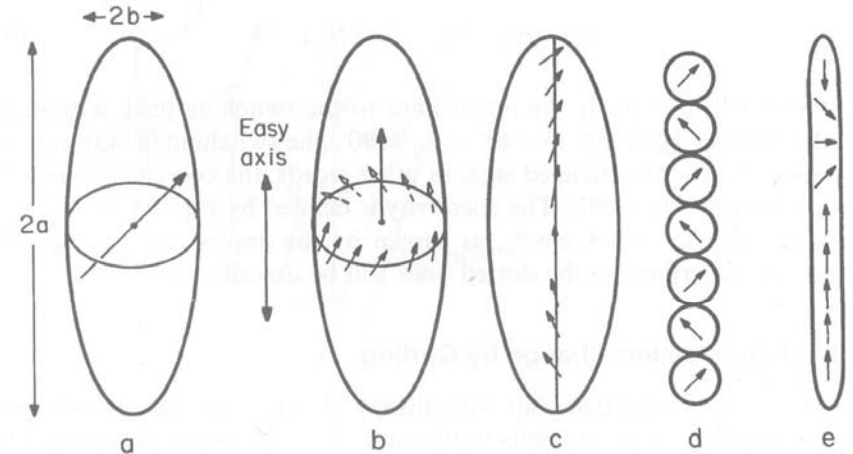
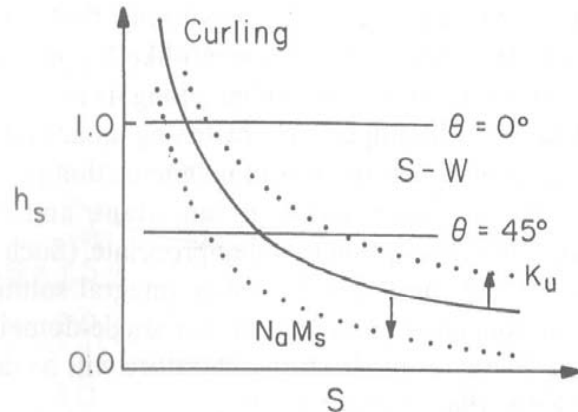


Figure 9.7. Modes of magnetization reversal in acicular fine particles. Left to right: (a) coherent rotation; (b) curling; (c) buckling; (d) fanning (in chain of spheres); and (e) domino effect. The first and third processes occur with the magnetization throughout the particle confined to a plane.

### (3) Magnetization Process



**Figure 9.8.** Schematic comparison of the switching fields for curling compared with the SW results shown for two angles of the field relative to the particle axis. Dotted lines for curling indicate that increased major-axis demagnetizing field  $N_a M_s$  favors curling; increased particle anisotropy inhibits curling.

- For smaller particles of superparamagnetism,

$$H_c \propto C_1 - C_2/b^{3/2}$$

As the particle volume decreases in the superparamagnetic regime,  $H_c$  drops at a given temperature. (see Fig. 9.9 in O'Handley)

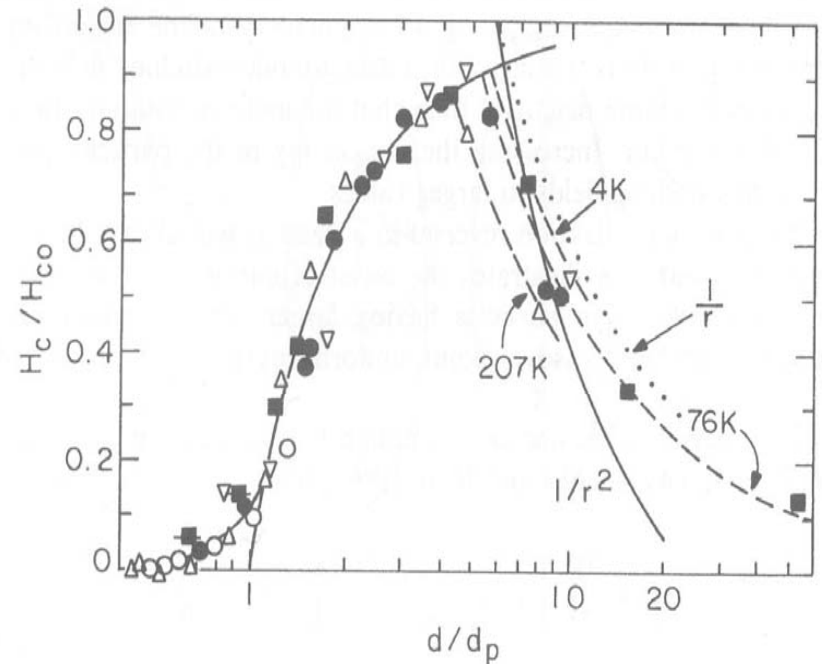


**Figure 9.9.** Particle-size variation of coercivity in FeCo particles (Kneller and Luborsky 1963). The solid negative-slope curve  $1/r^2$  follows Eq. (9.16). The solid positive-slope curve, starting at  $d/d_p = 1$ , is calculated from Eq. (9.17).

### (3) Magnetization Process

#### Free Domain Walls :

For large particles (or polycrystalline sample packed densely) with domain walls

- Assuming completely free domain walls :  $H_c = 0$

$M$ - $H$  characteristic for  $H > 0$  is the uniform rotation process

(see Fig. 9.10 in O'Handley)

#### Explanations :

- With decreasing  $H$  from positive saturation, domain walls are nucleated and move easily once  $H < 0$ .
- Both magnetization rotation and domain wall motion may contribute to the  $M$ - $H$  process.
- No magnetization reversal by abrupt rotational switching because of the easy wall motion.

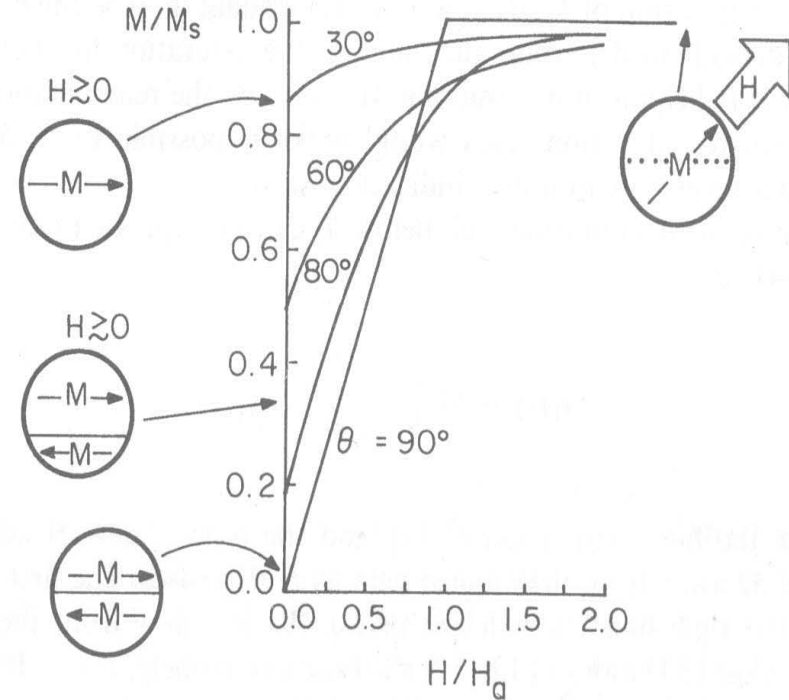


**Figure 9.10.** Reduced field versus reduced magnetization for a field applied at an angle  $\theta_0$  to the easy axis of particles significantly larger than the single-domain limit. The magnetization process is reversible both for magnetization rotation and for wall motion. Inserts depict possible magnetization configurations at various stages in the magnetization process (EA is horizontal in these inserts).

### (3) Magnetization Process

#### Approach to Saturation :

- **Experimental determination of  $M_s$**  is not always evident. In that case, the mathematical form of the approach to saturation is helpful. At  $T$  well below  $T_c$

$$M(H) = M_s(1 - a/H) + \chi_{hf}H$$

Here  $\chi_{hf}$  is the high-field susceptibility and the term  $-aM_s/H$  accounts for rotation of  $\mathbf{M}$  away from the applied field as  $H$  decreases. (see Fig. 9.11 in O'Handley)

- For single-domain particles, from the Stoner-Wohlfarth model, at the limit  $h \gg 1$ ,  $m \approx 1$  (or  $2m^2 - 1 \approx 1$ )

$$\pm 2h(1 - m^2)^{1/2} = (2m^2 - 1)\sin 2\theta_0$$

leading to  $m \approx (1 - \sin^2 2\theta_0/4h^2)^{1/2}$

and thus  $M(H) = M_s(1 - H_a^2 \sin^2 2\theta_0/8H^2)$

By extrapolating of  $M(H)$  vs  $H^{-2}$ ,  $M_s$  can be determined.

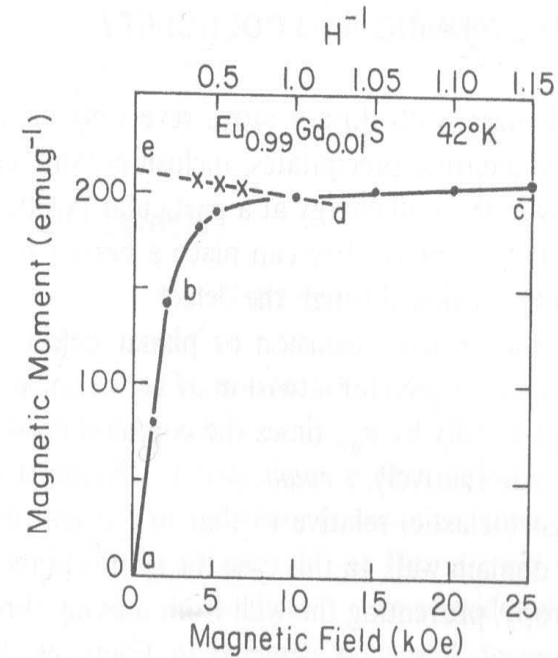


Figure 9.11. Method of determining saturation magnetization:  $M$  versus  $H$  and versus  $H^{-1}$  data for  $\text{Eu}_{0.99}\text{Gd}_{0.01}\text{S}$  at 4.2 K (McGuire and Flanders 1969).

### (3) Magnetization Process

#### □ Domain Wall Pinning and Coercivity

Why are domain wall motions irreversible in real materials under an external field  $H_{ext}$ ?

Domain wall energy can be lowered at a particular position in the material due to the defects such as grain boundaries, precipitates, inclusions, surface roughness, and other defects, and thus the wall motion can be effectively pinned or inhibited.

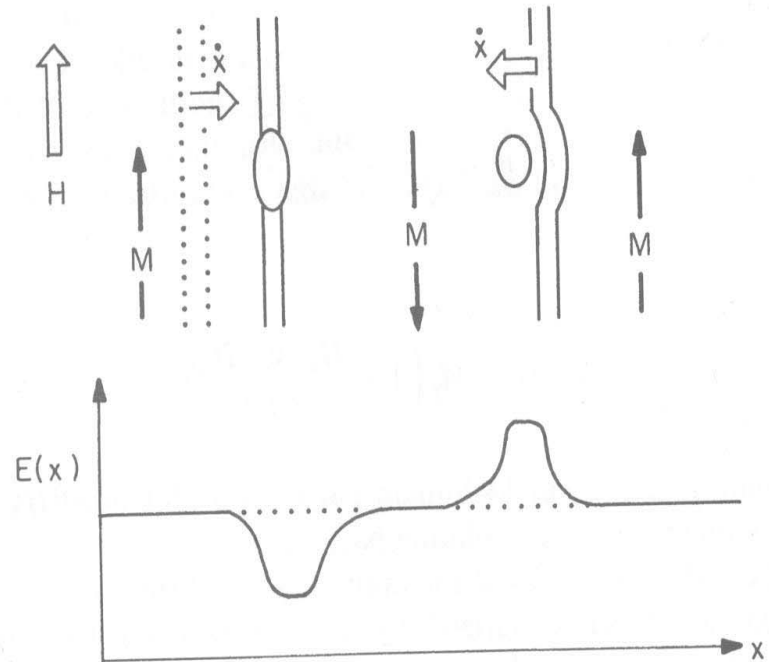


**Figure 9.12.** Upper panel depicts two kinds of defect and their influence on wall motion for vertical applied field: nonmagnetic inclusions locally lower the wall energy by decreasing its area; particles of different anisotropy or magnetization than the matrix present a barrier to wall motion. Below is shown the domain wall energy as a function of position in absence of an applied field.



## (3) Magnetization Process

- **Two classes of defect** (see Fig. 9.12 in O'Handley)

(i) **A nonmagnetic inclusion or planar defect coincident with a wall** : The need for a moment rotation (or a twist in  $\mathbf{M}$ ) across the defects is eliminated and thus the total wall energy can be locally reduced by  $\sigma_{dw}$  times the common cross-sectional area of the defect and wall.

(ii) **A magnetic defect having a strong anisotropy (crystalline or magnetoelastic) relative to that of the matrix** : Local wall energy is increased and thus a barrier to a domain wall motion can be posed effectively.

- **Distribution of defects in a material**

The domain wall potential  $\sigma_{dw}(x)$  is highly irregular with position.

The presence of the pinning defects leads to an irregular domain wall motion consisting of a series of Barkhausen jumps.

- **Quantitative models of domain wall motion**

Two regimes based on the ratio of defect size  $D$  to wall thickness  $\delta_{dw} = \pi(A/K_u)^{1/2}$ .

For  $D \gg \delta_{dw}$ , domain wall pinning on defects

(i) Large fuzzy defect case

(ii) Sharply defined defect case

### (3) Magnetization Process

**Large fuzzy defects** (see Fig. 9.13 in O'Handley) :  
strain fields or composition fluctuations

- The domain wall can be considered to be moving in an irregular but slowly changing potential
- The driving pressure due to the difference in Zeeman energy across a  $180^\circ$  wall :  $2M_s H$
- Resistance to the wall motion due to the gradient in the wall energy density :  $P = - d\sigma_{dw}/dx$

Then, since  $\sigma_{dw} = 4(AK_u)^{1/2}$  and  $K_u = K_{xtl} + (3/2)\lambda_s \sigma$

$$d\sigma_{dw}/dx = 4d(AK_u)^{1/2}/dx = 2[(\pi/\delta_{dw})\partial A/\partial x + (\delta_{dw}/\pi)(\partial K_{xtl}/\partial x + (3/2)\lambda_s \partial \sigma/\partial x)]$$

Explanations :

- Spatial variations in exchange and anisotropy energies, determining the wall energy, exert the impeding force to the domain wall motion.

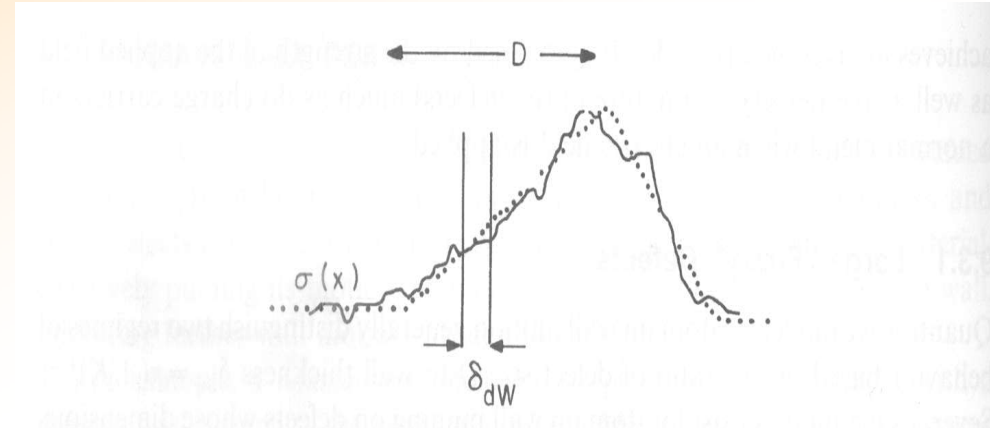


Figure 9.13. Domain wall thickness superimposed on a representation of the variation in wall energy density across a defect of full width at half maximum,  $D$ .



## (3) Magnetization Process

### Large fuzzy defects (continued)

The steepest gradient in wall energy density can be taken to be the magnetic pressure responsible for the coercivity  $H_c$

$$(d\sigma_{dw}/dx)_{\max} = 2M_s H_c \rightarrow H_c = (d\sigma_{dw}/dx)_{\max} / 2M_s$$

If the variation  $\sim D$ , and assuming a linear gradient,  $d\sigma_{dw}/dx = \Delta\sigma_{dw}/D$

$$H_c \approx (2H_a/)(\delta_{dw}/D)[\Delta A/A + \Delta K_{xtl}/K_{xtl} + (3/2)\lambda_s \Delta\sigma/K_{xtl}]$$

$H_c \propto \delta_{dw}/D$  times a sum of fluctuation terms expressing local variations in exchange stiffness, crystal anisotropy and magnetoelastic anisotropy, respectively.

where the anisotropy field,

$$H_a = 2K_{xtl}/M_s : \text{upper limit to the coercivity}$$

Coercive mechanism arising from the magnetostatic energy of defects proportional to  $\Delta M/M$

$$H_c \propto \Delta(2\pi M_s^2)/2\pi M_s^2 = 2\Delta M_s/M_s$$



### (3) Magnetization Process

#### Micromagnetic theory for well-defined defects

(see Fig. 9.14 in O'Handley)

Sharply defined defect case : grain boundaries, voids, antiphase boundaries, and dislocations

Total energy of the system in this model = exchange energy + uniaxial anisotropy energy + Zeeman energy densities

$$A_i(\partial\theta/\partial x)^2 + K_i\sin^2\theta - M_s H \cos\theta$$

where  $\theta$  = angle between magnetization and easy axis (y axis)

Over all space, minimum energy when

$$-2A_i(\partial\theta/\partial x)^2 + K_i\sin^2\theta - M_s H \cos\theta = C_i\theta$$

where  $i = 1, 2, 3$  corresponding to the regions in Fig. 9.14

Boundary conditions

$$d\theta/dx = 0 \text{ at } x = \pm \infty \text{ and}$$

$$\theta = 0 \text{ at } x = +\infty \text{ and } \theta = \pi \text{ at } x = -\infty$$

Therefore,  $C_1 = -HM_1$ ,  $C_3 = +HM_1$ ,  $C_2$  from continuity of  $\theta$  and exchange torque  $A_i d\theta/dx$  at the interfaces  $x_1$  and  $x_2$

Reduced coercive field  $h_c = H_c M_1 / K_1$

(see Fig 9.15 and 9.16 in O'Handley)

Summary (see Fig. 9.17 in O'Handley)

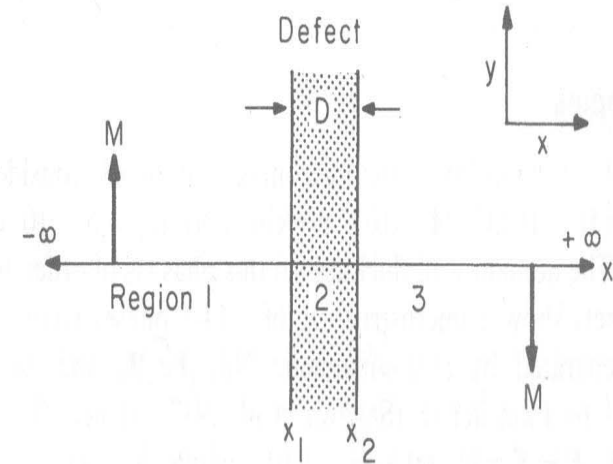
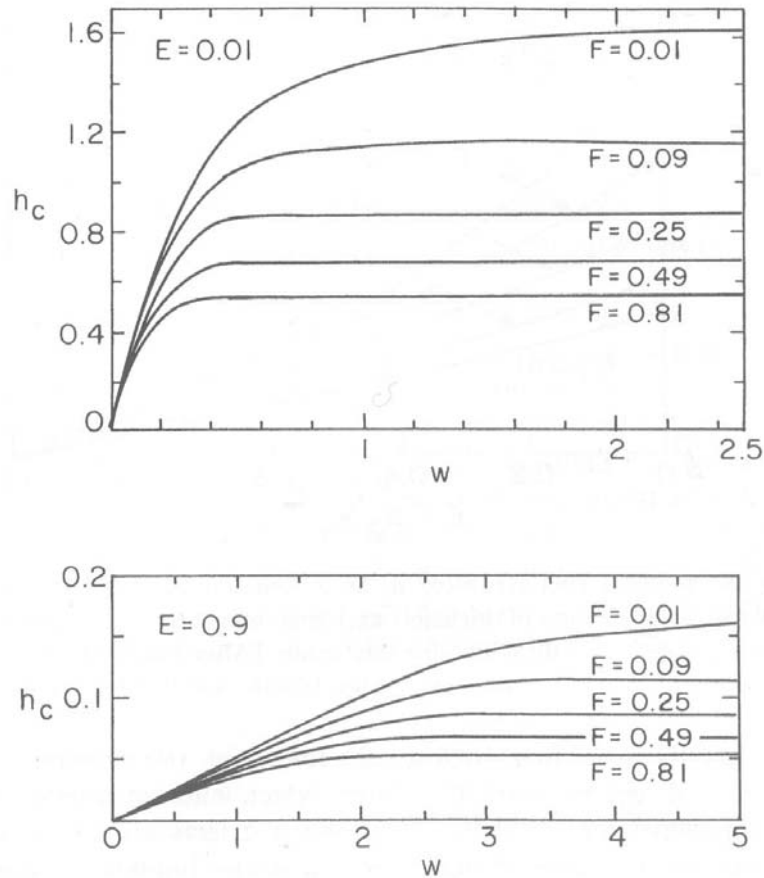
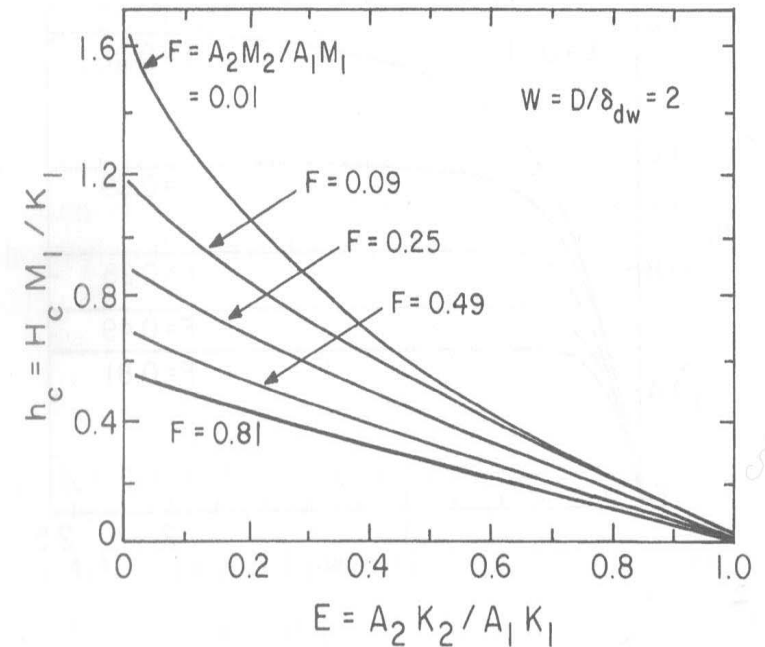


Figure 9.14. Division of a material into three regions: 1, to the left of a planar defect; 2, inside the planar defect; 3, to the right of the defect. Material properties are the same in regions 1 and 3. Defect width is  $D = x_2 - x_1$ , and magnetization values at  $\pm$ infinity indicate that a domain wall exists somewhere in between.

### (3) Magnetization Process



**Figure 9.15.** Reduced coercivity  $h_c$  versus normalized defect size  $w$  for various values of  $F$  and for small (above) and large (below) values of the square of the normalized defect wall energy density  $E$  (Paul 1982).



**Figure 9.16.** Normalized coercive force  $h_c$  as a function of the defect wall energy parameter  $E$  for various values of the defect exchange/magnetization stiffness parameter  $F$ . The normalized defect width is two for this figure. [After Paul (1982).]

### (3) Magnetization Process

#### Examples

- NdFeB (see Fig 9.18 in O'Handley)
- Amorphous and crystallized Co-Nb-B alloys (see Fig 9.19 in O'Handley)
- $\text{Sm}_2(\text{Co, Cu, Fe, Zr})_{17}$  (see Fig 9.17 in O'Handley)
- Nanoparticles (Chap 12 in O'Handley)

#### Additional Anisotropy

In some large single-domain particle systems (e.g., Fe in a  $\text{SiO}_2$  matrix), the coercivity can exceed the single-domain limit ( $2K/M_s$ ) due to an additional anisotropy (probably, stress or interfacial spin pinning) induced by the particle interaction with its nonmagnetic matrix.

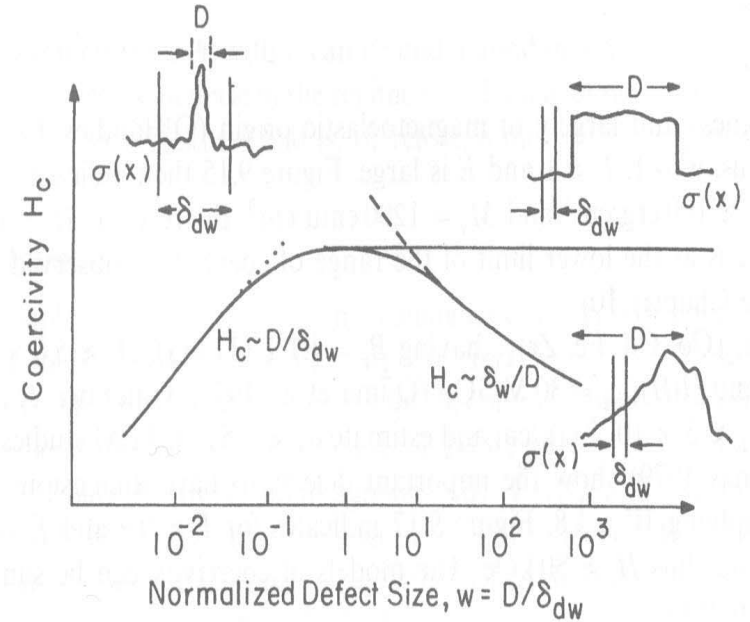


**Figure 9.17.** Schematic variation of coercivity with normalized defect size spanning two regions—small defects and large defects—relative to wall thickness. The predicted behavior in each case is shown.



## (3) Magnetization Process

### □ AC Processes

The area inside a  $B$ - $H$  loop = the energy loss per unit volume in one cycle

Energy  $W$  dissipated in a toroidal core over one cycle = the integral of the power loss over a period:

$$W = \int_{t=0}^{t=T} i(t) V(t) dt$$

Ampere's law and Faraday's law,  $V(t) = -d\phi/dt = -AdB/dt$

$$W = lA \int_{t=0}^{t=T} H \frac{dB}{dT} dt = lA \oint H(t) dB \quad : \text{DC hysteresis loss}$$

**Classical eddy-current loss**

**Eddy-current loss about a single domain wall**

**Multiple domain walls**

### □ Microwave Magnetization Dynamics & Ferromagnetic Resonance

How does the magnetization of a ferromagnetic material respond when the drive-field frequency approaches the natural precession frequency of the moment in a magnetic field?